EV-NVC: EFFICIENT VARIABLE BITRATE NEURAL VIDEO COMPRESSION

Yongcun Hu⁺, Yingzhen Zhai⁺, Jixiang Luo^{*}, Wenrui Dai, Dell Zhang, Hongkai Xiong, Xuelong Li^{*}

huyongcun61@gmail.com, zhaiyingzhen23@mails.ucas.ac.cn luojx14@chinatelecom.cn, daiwenrui@sjtu.edu.cn, dell.z@ieee.org, xionghongkai@sjtu.edu.cn, xuelong_li@ieee.org Institute of Artificial Intelligence (TeleAI), China Telecom

ABSTRACT

Training neural video codec (NVC) with variable rate is a highly challenging task due to its complex training strategies and model structure. In this paper, we train an efficient variable bitrate neural video codec (EV-NVC) with the piecewise linear sampler (PLS) to improve the rate-distortion performance in high bitrate range, and the long-short-term feature fusion module (LSTFFM) to enhance the context modeling. Besides, we introduce mixed-precision training and discuss the different training strategies for each stage in detail to fully evaluate its effectiveness. Experimental results show that our approach reduces the BD-rate by 30.56% compared to HM-16.25 within low-delay mode.

Index Terms— Neural video coding, variable bitrate, multi-stage training, long-short-term feature fusion

1. INTRODUCTION AND RELATED WORK

With the rapid development of short video platforms and self-media, there has been an explosive increase in the number of videos available on the internet. While over the past two decades, traditional video codecs have undergone significant development to meet evolving user demands, progressing from H.264/AVC [1] to H.265/HEVC [2], and then to H.266/VVC [3].

In recent years, convolutional neural network (CNN)-based end-to-end video compression algorithms have witnessed substantial advancements, achieving superior performance compared to traditional methods. These innovations can be traced back to the early development of end-to-end image compression algorithms [4, 5, 6], from which they have naturally evolved into the domain of video processing. Such algorithms can generally be classified into three main types: 3D autoencoder-based algorithms, residual coding-based algorithms, and conditional coding-based algorithms. The first category treats videos as a temporal sequence of images and extends the conventional 2D autoencoder used

in image compression to a 3D autoencoder [7, 8, 9], achieving video compression. Although this approach is relatively straightforward to implement, it typically demands large amounts of memory and computational resources. Residual coding-based algorithms [10, 11, 12] replace traditional codec components with neural networks. These methods utilize an optical flow extractor to estimate the optical flow between adjacent frames, which, along with the decoded previous frame, is used for warping to predict the current frame. The predicted frame is then combined with the encoded and transmitted residual to reconstruct the final frame. Rather than residual coding-based algorithms, conditional coding-based algorithms [13, 14, 15, 16] treat the decoded previous frame as condition information and calculate the reconstructed current frame implicitly using a conditional neural network. Thus, this approach is capable of achieving a lower entropy bound [17].

Conditional coding-based algorithms originate from [13] and have gained great attention in recent years. [18] not only preserves the reconstructed frames, but also retains intermediate features, which are used as additional information for encoding and decoding the subsequent frame. With incorporating multi-scale feature fusion during motion compensation, the method achieves performance comparable to VTM in low-delay mode. [15] introduces a group-based offset diversity technique to capture optical flow, while also incorporating a quadtree-based partitioning scheme within the entropy model. This combination effectively balances computational efficiency with accuracy, achieving performance comparable to that of ECM. [16] propose a variable rate strategy and a refresh mechanism, making it a variable rate SOTA model in low-latency coding.

Although neural video codecs have demonstrated high performance, several critical issues remain unresolved. Firstly, the majority of existing algorithms focus primarily on reconstructing the current frame based on either the previous frame or latent features, neglecting the integration of information from earlier frames or features. This limitation results in suboptimal reconstruction quality. Secondly, many of the existing models do not support variable rate, necessitating

¹⁺ Intern at TeleAI and equal contribution

^{2*} Corresponding author

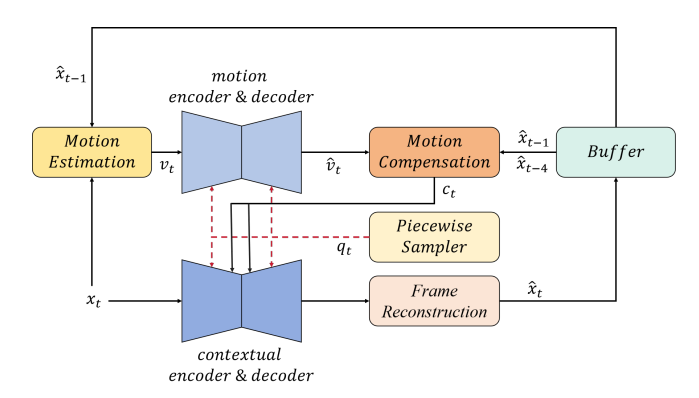


Fig. 1. Overview of the proposed method. x_t and \hat{x}_t are current and reconstructed frame. v_t and \hat{v}_t are motion vector and decoded motion vector. c_t is the conditional information. q_t is the rate control parameter.

multiple rounds of training and storage during operation, which leads to inefficient use of resources. Thirdly, while the aforementioned models typically require multi-stage training, there is a notable lack of comprehensive analysis regarding the specific training strategies applied at each stage. These absences significantly hamper the rapid reproduction and validation of these algorithms.

In this paper, we report EV-NVC, an open-source NVC integrating with a varible rate strategy, a long- and short-term fusion strategy, and a multi-stage training strategy. With these components, our EV-NVC outperforms VTM-17.0 in the YUV420 colorspace. Specifically, our contributions are:

- We propose a piecewise linear sampler (PLS) for training variable rate models, which effectively improves the rate-distortion performance in high bitrate range.
- We propose a long-short-term feature fusion module (LSTFFM), which reduces the BD-Rate by further fusing long-term information.
- We propose a multi-stage and mixed-precision training strategy and offer a compressive analysis of the objective functions and key parameters employed at each stage.

2. OVERVIEW OF OUR APPROACH

Fig. 1 illustrates the framework of the proposed method. For clarity, the entropy model is omitted. During training, we introduce PLS to generate the rate control parameter q. Compared to uniform sampling, this approach improves performance in the high bitrate range. The design of the sampler is discussed in Section 3.1. In terms of *motion compensation*, we employ LSTFFM to further integrate long-term information, as detailed in Section 3.2. For *motion estimation*, we adopt the pre-trained SpyNet [19]. The remaining components of the framework are consistent with DCVC-FM [16].

3. THE PROPOSED APPROACH

3.1. Piecewise Linear Sampler

Previous studies, such as [20], have observed performance degradation in the high bitrate range when training variable bitrate models using the same set of Lagrange multipliers adopted in fixed bitrate models. To address this issue, it was proposed that expanding the set of Lagrange multipliers to a larger range could mitigate this performance degradation. Inspired by this observation, we hypothesize that variable bitrate models operating in high bitrate and low bitrate ranges should not be treated equally during training. Models in a higher bitrate range are required to recover finer details, making their training more challenging. Therefore, we propose the following piecewise linear sampler.

$$p(idx) = \begin{cases} \frac{1}{1+m+m^2+m^3} & idx \in [1, \frac{n}{4}] \\ \frac{m}{1+m+m^2+m^3} & idx \in [\frac{n}{4}, \frac{n}{2}] \\ \frac{m^2}{1+m+m^2+m^3} & idx \in [\frac{n}{2}, \frac{3n}{4}] \\ \frac{m^3}{1+m+m^2+m^3} & idx \in [\frac{3n}{4}, n] \end{cases}$$
(1)

$$\lambda_{idx} = \lambda_{min} * \left(\frac{\lambda_{max}}{\lambda_{min}}\right)^{\frac{idx}{n}} \tag{2}$$

We sample different idx during training based on the probabilities in Eq. 1. The sampled idx is used to calculate the rate control parameter q. Specifically, we maintain a set of q_{min} and q_{max} , and perform exponential interpolation based on idx to obtain the current q. The Lagrange multiplier is calculated using Eq. 2, as [16]. In our implementation, the bitrate range is divided into four segments, with the sampling probability of each segment increasing according to a power function. The hyperparameters are configured as $m=2, n=64, \lambda_{min}=0.002, \lambda_{max}=0.25$ in our experiments.

3.2. Long-Short-Term Feature Fusion Module

We incorporate long-term information in a simple way without increasing the storage burden. Specifically, when encoding and decoding current frame x_t , we use not only previous frame \hat{x}_{t-1} , but also \hat{x}_{t-4} as reference information. We employ a long-short-term feature fusion module (LSTFFM) to perform feature fusion.

$$lt^t = \begin{cases} \hat{x}_0 & t < 4\\ \hat{x}_{t-4} & \text{else} \end{cases}$$
 (3)

Fig. 2 illustrates the structure of the LSTFFM. The right side of the module is the short-term feature extraction component, which corresponds to the multi-scale feature extraction mechanism in DCVC-FM [16]. This component is specifically designed to capture short-term information. On the left side, the input is processed in accordance with Eq. 3, utilizing a Feature Pyramid Network (FPN) [21] with residual connections to perform multi-scale feature extraction for long-term information. The long-term and short-term features are

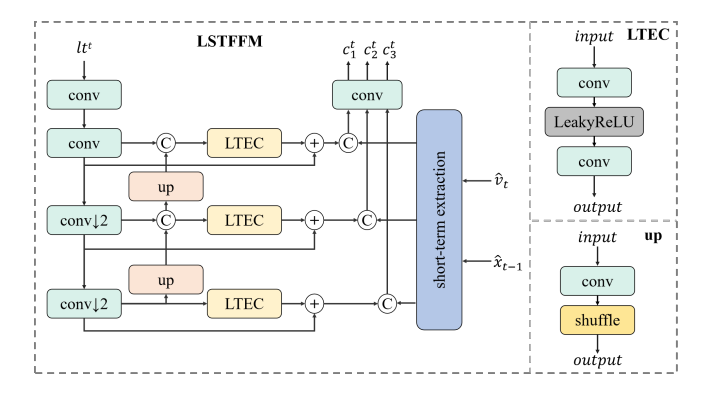


Fig. 2. The structure of long-short-term feature fusion module (LSTFFM). Long-term extraction conv (LTFC) adopts the conv-LeakyReLU-conv structure for further feature extraction, and upsampling module is implemented using conv and pixelshuffle. C is concatentation operation and $\downarrow 2$ is convolutional layer with stride 2.

then concatenated and passed through subsequent convolutional layers for feature fusion.

3.3. Multi-Stage Strategy

Our training strategy is depicted in Table 1. Following the work from [18] and [22], we adopt varying frame lengths, loss functions, and learning rates at different stages of training. We divide a video into four types: I, IP, PP, and IPP, and train these objectives sequentially. (1) I represents reconstructing I-frame. We use the I-frame model from [16]. Therefore, we do not train with single frame. (2) IP refers to reconstructing P-frames with reference to the I-frame. Therefore, we use two-frame input to train for this objective. (3) PP refers to reconstructing P-frames with reference to the previous P-frame. For this objective, a three-frame input is employed during training. Additionally, to match the compression losses inherent in longer sequences, four-frame and six-frame inputs are also used to train. (4) IPP refers to reconstructing the current P-frame with reference to the entire decoded sequence. Unlike the previous three loss types, this objective requires an RNN-based approach for training. Therefore, we use the longest possible sequence for training.

The rationale for using different frame lengths during training has been discussed above. In the following, we provide a detailed explanation of the selection of different loss functions. In the first four stages, we focus primarily on training the network parameters related to motion vectors with $loss_{meD}$ and $loss_{meRD}$, including the motion vector encoder, motion vector decoder, and the entropy model of motion vector. We use the decoded motion vectors \hat{mv} and the decoded previous frame \hat{x}_{t-1} to perform a warp operation to obtain the current predicted frame \hat{x}_t .

$$\hat{x}_t = Warp(\hat{x}_{t-1}, \hat{mv}) \tag{4}$$

Table 1. Multi-stage strategy.

stage	loss type	frames	lr	segment type		
stage1	meD	2	1e-4	IP		
stage2	meRD	2	1e-4	IP		
stage3	recD	2	5e-5	IP		
stage4	meRD	3	1e-4	PP		
stage5	recD	3	5e-5	PP		
stage6	recD	4	5e-5	PP		
stage7	recD	6	5e-5	PP		
stage8	recRD	2	5e-5	IP		
stage9	recRD	3	5e-5	PP		
stage10	recRD	4	5e-5	PP		
stage11	recRD	6	5e-5	PP		
stage12	all	2	5e-5	IP		
stage13	all	3	5e-5	PP		
stage14	all	4	5e-5	PP		
stage15	all	6	5e-5	PP		
stage16	all	6	1e-5	PP		
stage17	all	6	5e-6	PP		
stage18	avg	6	1e-5	IPP		

$$loss_{meD}^{t} = ||x_{t} - \hat{x}_{t}||_{2}^{2}$$
 (5)

$$loss_{meRD}^{t} = \lambda * loss_{meD}^{t} + bpp_{mv}^{t}$$
 (6)

From stage 5 to stage 10, we freeze network parameters related to motion vectors and train the remaining network parameters, further improving the video codec performance. At this time, the reconstructed frame \hat{x}_t is the output of the entire P-frame model.

$$loss_{recD}^{t} = \|x_t - \hat{x}_t\|_2^2 \tag{7}$$

$$loss_{recRD}^{t} = \lambda * loss_{recD}^{t} + bpp_{context}^{t}$$
 (8)

From stage 12 to stage 17, we train all network parameters. In stage 18, we adopt the multi-frame average loss.

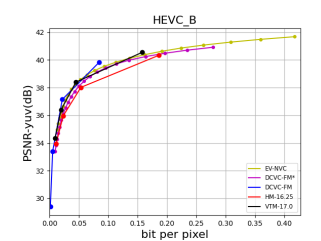
$$loss_{all}^{t} = loss_{recRD}^{t} + bpp_{mv}^{t}$$
 (9)

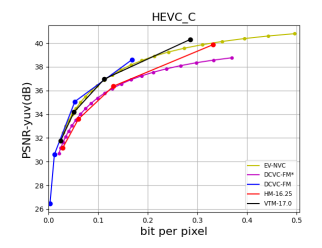
$$loss_{avg}^{T} = \frac{1}{T} \sum_{t=1}^{T} loss_{all}^{t}$$
 (10)

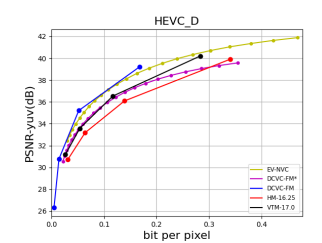
4. EXPERIMENTAL RESULTS

4.1. Experimental Setup

Datasets. We use Vimeo-90k setuplet dataset [23] for training, which contains 89800 video sequences and each with 7 frames at a resolution of 448×256 . The videos are randomly cropped into 256×256 patchs. We use RTX 4090 for training, and due to memory limitations, we do not employ additional datasets for fine-tuning. For testing, we use HEVC Class B, C, D [24].







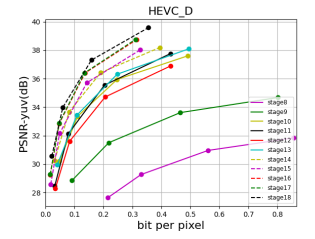


Fig. 3. Rate-distortion curves for HEVC Class B, C, D. The comparison is in YUV420 colorspace. PSNR (6*PSNRY + PSNRU + PSNRV)/8 is used to evaluate the distortion of the decoded pictures. The most right figure is the rate-distortion curve for HEVC Class D from stage8 to stage18.

Table 2. BD-Rate(%) comparison in YUV420 colorspace measured with PSNR. 96 frames with intra-period=–1. The anchor is HM-16.25.

	В	С	D	avg
HM-16.25	0.0	0.0	0.0	0.0
VTM-17.0	-28.38	-27.23	-24.53	-26.71
DCVC-FM*	-6.70	-1.76	-21.86	-10.11
EV-NVC	-23.49	-27.41	-40.79	-30.56

Test condition. We test 96 frames for each video in YUV420 colorspace. The intra period is set to -1 rather than 32. Our benchmarks include HM-16.25 [25], VTM-17.0 [26] and DCVC-FM*. DCVC-FM* is the result we train DCVC-FM from scratch, and can be treated a variant of EV-NVC without PLS and LSTFFM, serving as the baseline in the ablation study.

We use the Adam [27] optimizer and training each stage for 20 epochs following the Table 1. To further accelerate training and reduce memory consumption, we employ mixed-precision training. We use BD-Rate [28] to quantify compression efficiency variations, where negative values correspond to bitrate savings and positive values indicate increased bitrate requirements.

4.2. Comparisons With Other Methods

Table 2 shows the comparison for YUV420 colorspace under 96 frames with intra-period -1. Our EV-NVC BD-Rate saving over HM and VTM is 30.56% and 3.85%, respectively. Despite the removal of PLS and LSTFFM, our DCVC-FM* still achieves a 10.11% reduction in BD-Rate compared to HM, due to the proposed training strategy.

Fig. 3 shows the rate-distortion curves. The proposed EV-NVC is capable of selecting a total of 64 RD points and we select one point every four points to plot the curves. The idx of RD points in DCVC-FM [16] are $\{0, 21, 42, 63\}$. As observed in the figure, EV-NVC covers a high bitrate range and fully encompasses the bitrate range used by HM and VTM. In addition, it exhibits a performance curve that closely aligns with that of VTM on Class B and C, while exhibiting a sig-

Table 3. Ablation study for our method.

PLS	LSTFFM	В	С	D	avg
Х	Х	0.0	0.0	0.0	0.0
1	×	-4.91	-9.24	-9.39	-7.85
X	✓	-8.52	-10.81	-9.44	-9.59
✓	✓	-23.49	-27.41	-40.79	-30.56

nificant improvement over VTM on Class D. Furthermore, the performance curve of the proposed method is highly comparable to that of DCVC-FM [16], despite utilizing a maximum of six frames for training, whereas the latter incorporates an additional 32 frames for post-finetuning.

4.3. Ablation Study

We have demonstrated the training effects of using different loss functions, varying frame lengths, learning rate, and segment type at different stages in the most right figure of Fig. 3, which is the rate-distortion curve for HEVC Class D from stage8 to stage18. For stage8 to stage11, we use $loss_{recRD}$ as the loss function with input frames from 2 to 6 and increasing input frames significantly improves the performance. For stage12 to stage15, we use $loss_{all}$ and observe the similar phenomenon. In addition, stage18 shows a significant performance improvement over stage17.

Table 3 presents the results of the ablation study on the PLS and LSTFFM. The experimental results demonstrate that the incorporation of the PLS leads to a 7.85% reduction in BD-Rate, while the inclusion of LSTFFM results in a 9.59% reduction. When both components are utilized together, the BD-Rate reduction reaches 25.03%.

5. CONCLUSION

EV-NVC reveals the process of training end-to-end video compression with only maximal six frames and mixed-precision training, and it also introduces PLS and LSTFFM to reduce computational complexity and enchance the context model. Besides EV-NVC will contribute to the advancement of AI flow, which can make AI flow across variable devices.

6. REFERENCES

- [1] Thomas Wiegand, Gary J Sullivan, Gisle Bjontegaard, and Ajay Luthra, "Overview of the h. 264/avc video coding standard," *IEEE Transactions on circuits and systems for video technology*, vol. 13, no. 7, pp. 560–576, 2003.
- [2] Gary J Sullivan, Jens-Rainer Ohm, Woo-Jin Han, and Thomas Wiegand, "Overview of the high efficiency video coding (hevc) standard," *IEEE Transactions on circuits and systems for video technology*, vol. 22, no. 12, pp. 1649–1668, 2012.
- [3] Benjamin Bross, Ye-Kui Wang, Yan Ye, Shan Liu, Jianle Chen, Gary J Sullivan, and Jens-Rainer Ohm, "Overview of the versatile video coding (vvc) standard and its applications," *IEEE Transactions on Circuits and Systems for Video Technology*, vol. 31, no. 10, pp. 3736– 3764, 2021.
- [4] Johannes Ballé, Valero Laparra, and Eero P Simoncelli, "End-to-end optimized image compression," *arXiv* preprint arXiv:1611.01704, 2016.
- [5] Johannes Ballé, David Minnen, Saurabh Singh, Sung Jin Hwang, and Nick Johnston, "Variational image compression with a scale hyperprior," arXiv preprint arXiv:1802.01436, 2018.
- [6] Jixiang Luo, "Rethinking learned image compression: context is all you need," *arXiv preprint arXiv:2407.11590*, 2024.
- [7] Amirhossein Habibian, Ties van Rozendaal, Jakub M Tomczak, and Taco S Cohen, "Video compression with rate-distortion autoencoders," in *Proceedings of the IEEE/CVF International Conference on Computer Vi*sion, 2019, pp. 7033–7042.
- [8] Jorge Pessoa, Helena Aidos, Pedro Tomás, and Mário AT Figueiredo, "End-to-end learning of video compression using spatio-temporal autoencoders," in 2020 IEEE Workshop on Signal Processing Systems (SiPS). IEEE, 2020, pp. 1–6.
- [9] Wenyu Sun, Chen Tang, Weigui Li, Zhuqing Yuan, Huazhong Yang, and Yongpan Liu, "High-quality single-model deep video compression with frameconv3d and multi-frame differential modulation," in Computer Vision–ECCV 2020: 16th European Conference, Glasgow, UK, August 23–28, 2020, Proceedings, Part XXX 16. Springer, 2020, pp. 239–254.
- [10] Zhihao Hu, Guo Lu, and Dong Xu, "Fvc: A new framework towards deep video compression in feature space,"

- in Proceedings of the IEEE/CVF Conference on Computer Vision and Pattern Recognition, 2021, pp. 1502–1511.
- [11] Eirikur Agustsson, David Minnen, Nick Johnston, Johannes Balle, Sung Jin Hwang, and George Toderici, "Scale-space flow for end-to-end optimized video compression," in *Proceedings of the IEEE/CVF Conference on Computer Vision and Pattern Recognition*, 2020, pp. 8503–8512.
- [12] Yibo Shi, Yunying Ge, Jing Wang, and Jue Mao, "Alphave: High-performance and efficient learned video compression," in *European Conference on Computer Vision*. Springer, 2022, pp. 616–631.
- [13] Jiahao Li, Bin Li, and Yan Lu, "Deep contextual video compression," *Advances in Neural Information Processing Systems*, vol. 34, pp. 18114–18125, 2021.
- [14] Jiahao Li, Bin Li, and Yan Lu, "Hybrid spatial-temporal entropy modelling for neural video compression," in *Proceedings of the 30th ACM International Conference on Multimedia*, 2022, pp. 1503–1511.
- [15] Jiahao Li, Bin Li, and Yan Lu, "Neural video compression with diverse contexts," in *Proceedings of the IEEE/CVF Conference on Computer Vision and Pattern Recognition*, 2023, pp. 22616–22626.
- [16] Jiahao Li, Bin Li, and Yan Lu, "Neural video compression with feature modulation," in *Proceedings of the IEEE/CVF Conference on Computer Vision and Pattern Recognition*, 2024, pp. 26099–26108.
- [17] Théo Ladune, Pierrick Philippe, Wassim Hamidouche, Lu Zhang, and Olivier Déforges, "Optical flow and mode selection for learning-based video coding," in 2020 IEEE 22nd International Workshop on Multimedia Signal Processing (MMSP). IEEE, 2020, pp. 1–6.
- [18] Xihua Sheng, Jiahao Li, Bin Li, Li Li, Dong Liu, and Yan Lu, "Temporal context mining for learned video compression," *IEEE Transactions on Multimedia*, vol. 25, pp. 7311–7322, 2022.
- [19] Anurag Ranjan and Michael J Black, "Optical flow estimation using a spatial pyramid network," in *Proceedings of the IEEE conference on computer vision and pattern recognition*, 2017, pp. 4161–4170.
- [20] Kedeng Tong, Yaojun Wu, Yue Li, Kai Zhang, Li Zhang, and Xin Jin, "Qvrf: A quantization-error-aware variable rate framework for learned image compression," in 2023 IEEE International Conference on Image Processing (ICIP). IEEE, 2023, pp. 1310–1314.

- [21] Tsung-Yi Lin, Piotr Dollár, Ross Girshick, Kaiming He, Bharath Hariharan, and Serge Belongie, "Feature pyramid networks for object detection," in *Proceedings of the IEEE conference on computer vision and pattern recognition*, 2017, pp. 2117–2125.
- [22] Xihua Sheng, Chuanbo Tang, Li Li, Dong Liu, and Feng Wu, "Nvc-1b: A large neural video coding model," arXiv preprint arXiv:2407.19402, 2024.
- [23] Tianfan Xue, Baian Chen, Jiajun Wu, Donglai Wei, and William T Freeman, "Video enhancement with task-oriented flow," *International Journal of Computer Vision*, vol. 127, pp. 1106–1125, 2019.
- [24] Frank Bossen et al., "Common test conditions and software reference configurations," *JCTVC-L1100*, vol. 12, no. 7, pp. 1, 2013.
- [25] "Hm," https://vcgit.hhi.fraunhofer.de/
 jvet/HM/.
- [26] "Vtm," https://vcgit.hhi.fraunhofer.de/ jvet/VVCSoftware_VTM/.
- [27] Diederik P Kingma, "Adam: A method for stochastic optimization," *arXiv preprint arXiv:1412.6980*, 2014.
- [28] G Bjontegaard, "Calculation of average psnr differences between rd-curves," *ITU-T SG16 Q*, vol. 6, 2001.